energies

MDPI

Article

Autothermal Siberian Pine Nutshell Pyrolysis Maintained by Exothermic Reactions

Alexander Astafev [1,2], Ivan Shanenkov [1], Kanipa Ibraeva [1], Roman Tabakaev [1,2,*] and Sergei Preis [3]

[1] Institute of Environmental and Agricultural Biology (X-BIO), University of Tyumen, 6 Volodarskogo Street, 625003 Tyumen, Russia
[2] School of Energy and Power Engineering, National Research Tomsk Polytechnic University, 30 Lenina Avenue, 634050 Tomsk, Russia
[3] Department of Materials and Environmental Technology, Tallinn University of Technology, 5 Ehitajate Tee, 19086 Tallinn, Estonia
* Correspondence: tabakaevrb@tpu.ru

Abstract: The global energy industry works towards an increased use of carbon-neutral biomass. Nutshell represents a regional bio-waste, i.e., a bio-energy resource. Pyrolysis is a common method for processing biomass into valuable energy products. The heat demand, however, limits pyrolysis applications. Yet, such demand may be addressed via exothermic pyrolysis reactions under selected operation conditions. Making the pyrolysis of Siberian pine nutshell autothermic comprised the objective of the study. The study involved analytical methods together with a pyrolysis experiment. The analytical methods included a thermogravimetric analysis combined with differential scanning calorimetry and an integrated gas analyzer. Thermophysical characterization was executed using a thermal diffusivity analyzer with the laser flash method. At 650 °C, pyrolytic heat was released in the amount of 1224.6 kJ/kg, exceeding the heat demand of 1179.5 kJ/kg. Pyrolysis at a lower temperature of 550 °C remained endothermic, although the combusted gas product provided 847.7 kJ/kg of heat, which, together with exothermic release, covered the required heat demand for the pyrolysis process.

Keywords: pyrolysis; pine nutshell; exothermic reactions; heat expense; pyrolysis gas

check for updates

Citation: Astafev, A.; Shanenkov, I.; Ibraeva, K.; Tabakaev, R.; Preis, S. Autothermal Siberian Pine Nutshell Pyrolysis Maintained by Exothermic Reactions. *Energies* **2022**, *15*, 7118. https://doi.org/10.3390/en15197118

Academic Editors: Lisandra Rocha Meneses, Abrar Inayat and Timo Kikas

Received: 7 September 2022
Accepted: 23 September 2022
Published: 28 September 2022

Publisher's Note: MDPI stays neutral with regard to jurisdictional claims in published maps and institutional affiliations.

Copyright: © 2022 by the authors. Licensee MDPI, Basel, Switzerland. This article is an open access article distributed under the terms and conditions of the Creative Commons Attribution (CC BY) license (https://creativecommons.org/licenses/by/4.0/).

1. Introduction

In recent years, the reduction in greenhouse gas emissions for carbon neutrality in heat and electricity production has become an increasingly urgent task [1–3]. The latest regulatory documents in environmental protection set the goal for the world community to strive for a balance between carbon dioxide emissions and their absorption or utilization [4,5]. The achievement of this goal in different countries is closely related to their energy security. One of the options providing a two-way solution to this problem is the application of local renewable sources of heat and electricity, namely biomass; being a natural sink of CO_2, it meets the zero-emission requirement [6]. Together with the fact that biochar produced in pyrolysis improves soil quality and the life cycle of plants, the thermal processing of biomass provides a promising approach to its utilization [7,8]. Moreover, being evenly distributed geographically, biomass waste has potential as an equitable energy storage vehicle [9]. The production of biomass waste is increasing, together with the productivity of agricultural and timber processing enterprises [10,11]. As a rule, biomass processing enterprises are located in close proximity to settlements with a decentralized energy supply, meaning that bio-waste utilization for valuable energy products supports regional energy security. The competent use of bio-resources provides both autonomy in terms of energy supplies and a reduction in greenhouse gas emissions. The factors limiting the role of biomass in the energy balance include high humidity, low density, heterogeneity in composition, and the slagging of some species. Among the efficient methods for improving energy storage in biomass, pyrolysis is the most promising, according to the literature [12].

This method is virtually a waste-free technology because all the products are applicable for energy supplies or in other industries. For example, the yield of high-calorific gas may be increased on account of the tars minimized in catalytic cracking, while biochar residue may be used as an adsorbent. The yield of biochar, in turn, may be increased by using pyrolysis gas to heat the retort [13]; the liquid products can be used in the production of biofuels [14] or as a raw material in chemical synthesis [15].

A well-known review article [16] presents data on the ambiguity of the total thermal effect of pyrolysis, varying from endothermic to exothermic. Numerous studies have reported biomass pyrolysis as endothermic [17,18]. However, exothermic processes have also been proven [19–22] for individual biomass particles and small weights, using analytical methods of differential scanning calorimetry (DSC) [23,24]. In addition, there are methods of enthalpy estimation for the feedstock and products [25], as well as for the determination of pyrolysis activation energy [26]. The exothermic effect of wood pyrolysis, with large tolerances in either direction, may be estimated at 1000 kJ/kg [27]. The Strache diagram shows that the thermal effect of decomposition in the semi-coking process grows with increased oxygen content in the fuel composition, reaching a maximum at 45% wt. O_2 and decreasing beyond that point [28]. Low-temperature pyrolysis proceeding at temperatures similar to that of semi-coking (500–550 °C) demonstrated a similar dependence of the thermal effect on the content of oxygen. On a large scale, the retort's temperature maintenance was experimentally observed when the external heating was turned off at a certain temperature [29]. The work in [30] describes a plant for producing charcoal by the pyrolysis method, in which the raw material is heated from 350 to 500 °C using the heat released by exothermic reactions.

The autothermic character of pyrolysis makes it extremely attractive both technically and economically. For the development of pyrolysis in this direction, the proper conditions to ensure that the heat released from exothermic reactions exceeds the heat absorbed by endothermic ones must be selected. For the moment, a number of works have established the total thermal effect of pyrolysis for, e.g., four types of biomass and their constituents cellulose, xylan, and lignin [31]; these works provide equations describing the thermal effect dependent on the conversion degree of the biomass. The course of pyrolysis, i.e., the quantitative ratio of the products, and its thermal effect are affected by the biomass composition and the process parameters. For example, di Blasi et al. [32] established the relationship between the humidity of hazelnut shell and the heat effect of its pyrolysis. A number of works described the effect of the process parameters on the total heat released in the pyrolysis zone during the residence time of volatile products [33,34] and the yield of carbonaceous residue [35,36]. These works concluded that longer secondary reactions between volatile products and the carbonaceous residue resulted in an increased yield of the latter and an exothermic effect.

Autothermic pyrolysis requiring external energy only for its initiation was implemented for the first time in the Stafford retort at the beginning of the 20th century [37]. For biomass applications, autothermic pyrolysis was developed in several directions, e.g., oxidative pyrolysis [38–40], in which an oxidizing agent is added to the reactor or its section instead of an inert gas providing exothermic reactions. Another kind of autothermic pyrolysis utilizes the heat of interacting fluidized beds in biomass fast pyrolysis: the biomass is fed into the inner tube of the reactor in the stream of the inert or pyrolysis gas; then, the inner tube is heated by the fluidized bed combustion of pyrolysis carbonaceous residue in the outer tube with the addition of sand and a catalyst [41,42]. Pyrolysis gas combustion also provides heat implemented at an industrial scale in BioThermTH fluidized bed pyrolysis (DynaMotive Technologies, Richmond, BC, Canada) [43].

Layered pyrolysis reactors are the most widespread for their reliability and simplicity in construction and operation. This makes their adjustment to autothermic exploitation an urgent research task for biomass pyrolysis reactors. To do this, a thoroughly studied heat balance is necessary in terms of the components of energy generation, including the heat

of exothermic reactions and the combustion of the pyrolysis gas, as well as consumption, including external heat for the process implementation.

2. Materials and Methods

2.1. Research Object

Siberian pine nutshell, widespread in the Siberian Federal District, was considered as the research object. The main thermal characteristics of the Siberian pine shell were determined by certified methods: ISO 1171:2010 for the ash content, ISO 11722:2013 for moisture, and ISO 562:2010 for volatile compounds. The combustion heat was determined according to ISO 1928:2020 using the ABK-1 bomb calorimeter (RET, Moscow, Russia). The elemental composition was established using a Vario Micro Cube analyzer (Elementar, Langenselbold, Germany). The characteristics of carbonaceous residue and tars were determined similarly to those of the raw material, while the combustion heat of the gas was calculated according to its composition. The thermal stability coefficient, which characterizes the resistance of the fuel to heating, was found using Equation (1):

$$\text{Thermal stability (TS)} = \frac{\text{FC}}{\text{FC} + \text{VM}} \quad (1)$$

where FC is a fixed carbon content, % and VM is the volatile matter content, %.

Table 1 shows the characteristics of the Siberian pine nutshell and the products of its pyrolysis, i.e., solid carbonaceous residue and liquid tar. The obtained data are consistent with those reported earlier [44]. For the natural raw material, as for all other types of biomass, typical values for the yield of volatile substances and carbon content, as well as low ash content and high calorific values, were observed. At the same time, there are studies reporting high contents of potassium in the ash residue of pine nutshell [44,45], which is the added value of this biomass as a key and widely used nutrient for plant vegetation [46].

Table 1. Proximate and ultimate analysis of Siberian pine nutshell and products of pyrolysis.

Parameter	Raw Material	Carbonaceous Residue	Tar
Moisture W^{a},%	13.0	2.2	N.a.
Ash content on dry basis A^{d},%	1.0	1.5	0.0
Volatile matter yield V^{daf},%	69.7	22.0	100.0
Low calorific value Q_i^r, MJ/kg	18.1	28.3	27.5
Elemental composition on dry ash-free weight, %			
C^{daf}	51.81	82.37	64.60
H^{daf}	6.39	3.70	7.06
N^{daf}	0.24	0.53	0.64
S^{daf}	traces	traces	traces
O^{daf}	41.56	13.40	27.70
Coefficient of thermal stability (Equation (1))	0.43	0.79	N.a.

N.a.—not applicable; ^{a}—analyzed basis; ^{d}—dry basis; ^{r}—received basis; ^{daf}—dry ash-free basis.

Biochar having a high calorific value, comparable to some types of coals, may be used as a fuel or an adsorbent since the solid residue is usually a material with high porosity and adsorption capacity. A low sulfur content is a prerequisite for low emissions of SO_2 in the energy-related use of the raw material and its pyrolysis products. The thermal stability of carbonaceous residue is almost two times higher than that of nutshell, which is associated

with decreased fuel reactivity: the V^{daf} value of the solid residue is more than three times lower than that of the nutshell.

2.2. Characterization of Experimental Techniques

The pyrolysis material balance was compiled according to ISO 647:2017 from the results obtained by using the laboratory setup shown in Figure 1. A detailed experiment description and the data processing method were described previously [47].

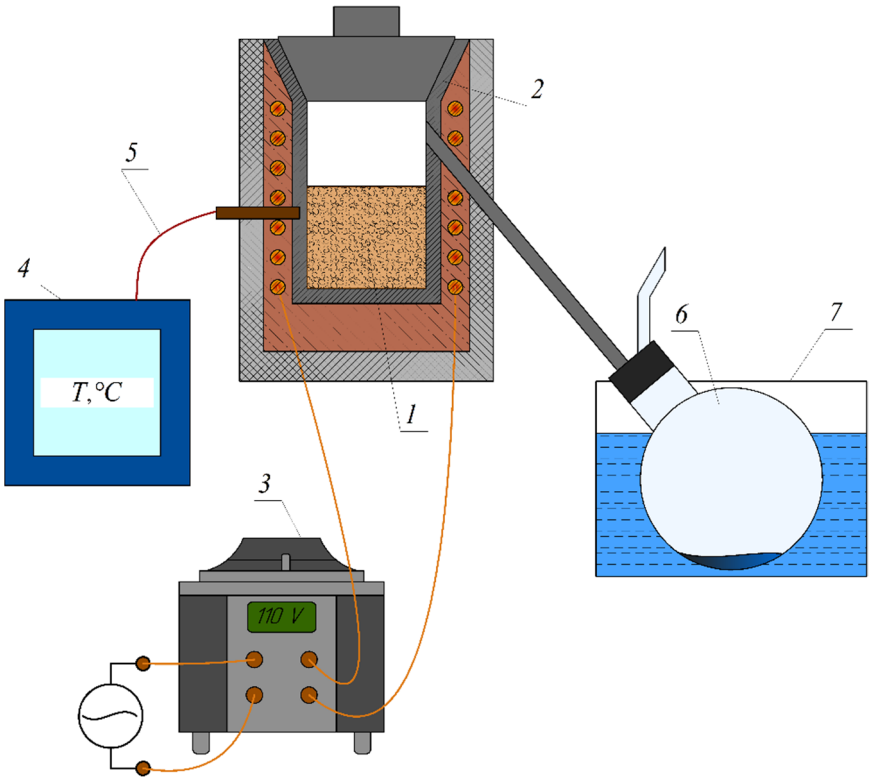


Figure 1. Laboratory installation for determining the yield of pyrolysis products: 1—Siberian pine nutshell, 2—reactor, 3—laboratory transformer, 4—high-precision multichannel temperature meter TM 5104 (Elemer, Russia), 5—K-type thermocouple, 6—receiver flask, 7—cooling water bath.

The energy content of the pyrolysis products relative to the initial biomass was calculated using Equation (2):

$$\text{Energy yield (EY)} = \frac{m_i \times (Q_i^d)_i}{m_0 \times (Q_i^d)_0} \times 100, \% \quad (2)$$

where m_i is the mass of the dry pyrolysis product, kg; m_0 is the initial mass of the dry raw material, kg; $(Q_i^d)_i$ is the calorific value of the pyrolysis product, MJ/kg; and $(Q_i^d)_0$ is the calorific value of the raw material, MJ/kg.

The fuel humidity depends on the environmental conditions, including air humidity, temperature, and atmospheric pressure. The authors present an approach implemented for dried fuel. The characteristics of pine nutshell, as well as the resulting products, were converted to dry weight: for example, the value Q_i^d used in Equation (2) was calculated according to the data given in Table 1 using Equation (3):

$$Q_i^d = \frac{100}{100 - W^a} \times Q_i^r \quad (3)$$

The share of the energy yield obtained with pyrolysis gas was calculated as residual from the heat balance (Equation (4)), while the pyrogenetic water was taken as a zero-calorie product:

$$EY(gas) = 1 - EY(c.r.) - EY(tar), \% \quad (4)$$

The thermal effects during the decomposition of the raw material and the components of the gaseous products were determined by means of thermogravimetric analysis (TGA) combined with differential scanning calorimetry (DSC). This analysis was performed using the STA 449 F5 Jupiter microthermal analyzer with an integrated QMS 403 Aeolos gas analyzer (NETZSCH, Selb, Germany) in an argon atmosphere (with a carrier gas flow of 50 mL/min), simulating the conditions of pyrolysis without oxidation reactions. To perform the experiment, the raw material was brought to an air-dry state, after which it was ground using a VLM-25 laboratory mill (Vilitek, Moscow, Russia) and screened through the Analysette 3 SPARTAN vibrating sieve (Fritsch, Idar-Oberstein, Germany). For analysis, a fraction below 0.2 mm was used to increase the homogeneity of the test sample and reduce the impact of air in the voids on the thermal effects. Samples of 20 mg were used in a temperature range from 20 to 900 °C at the heating rate of 10 °C/min. The gaseous products were transported to the quadrupole mass spectrometer through a transfer line heated to 235 °C to prevent condensation. The mass spectra were recorded with a step of 1 for the 1 to 50 amu interval.

The heat release (relative to 1 kg of dry raw material) in pyrolysis was determined by two methods: (i) by analyzing the obtained results in the NETZSCH Proteus software and (ii) by comparing the area of the endothermic minimum associated with the moisture evaporation S_{endo} with the areas of the exothermic maxima of the organic share of the raw material S_{exo}, as in Equation (5):

$$Q_{exo} = Q_{endo} \times \frac{S_{exo}}{S_{endo}} \times \frac{100}{100 - W}, kJ/kg \quad (5)$$

where Q_{endo} is the endothermic peak value, as determined in Equation (6):

$$Q_{endo} = c_p \times \frac{W}{100} \times (t_1 - t_0) + \frac{W}{100} \times r, kJ/kg \quad (6)$$

where c_p is the heat capacity of water vapor equal to 4.187 kJ/(kg·°C); W is the moisture in the raw material, %; t_0 is the initial temperature equal to 20 °C; t_d is the temperature of complete external moisture evaporation equal to 120 °C; and r is the heat of vaporization equal to 2258.2 kJ/kg.

The areas S_{exo} and S_{endo} were determined using the KOMPAS 3D V16 software.

The heat expense for pyrolysis, including the heat consumed by the formation and evaporation of moisture Q_{endo}, is associated with the heating of biomass to a temperature t_1, at which its decomposition begins Q_2 (Equation (7)), further heating until the process ends (t_p), and the feedstock is converted into carbon residue Q_3, (Equation (8)), as well as with the heat content in pyrolysis volatile products Q_4 (Equation (9)):

$$Q_2 = \left(1 - \left(\frac{W}{100}\right)\right) \times C_{p_b} \times (t_1 - t_0), kJ/kg \quad (7)$$

$$Q_3 = 0.5 \times \left(1 - \left(\frac{W}{100}\right)\right) \times (t_p - t_1) \times C_{p_{cr}} \times (\omega_{cr1} + \omega_{crp}), kJ/kg \quad (8)$$

$$Q_4 = 0.5 \cdot \left(1 - \left(\frac{W}{100}\right)\right) \times (t_p - t_1) \times C_{p_{vol}} \times \left(\omega_{vol1} + \omega_{volp}\right), kJ/kg \quad (9)$$

where C_{p_b}, $C_{p_{cr}}$ are the heat capacities of the initial biomass and the carbon residue, respectively, determined using a DLF-1200 thermal diffusivity analyzer (TA Instruments, New Castle, DE, USA) by the laser flash method described in [48], kJ/(kg·°C) $C_{p_{vol}}$ is the heat capacity of the volatile pyrolysis products determined as described in [49] according to their

condensable tar, pyrogenic water, and non-condensable gaseous components, kJ/(kg·°C); t_1 is the temperature at which biomass active decomposition begins, as determined in the TGA/DSC analysis, °C; t_p is the end pyrolysis temperature, °C; ω_{cr1}, ω_{crp}, ω_{vol1}, ω_{volp} are the shares of carbonaceous residues and volatile pyrolysis products at temperatures t_1 and t_p, respectively, %.

When compiling the heat balance of biomass processing, the heat content (HC) in the carbon residue and tar were calculated using Equation (10):

$$HC_i = \frac{m_i}{m_0} \times (Q_i^d)_0, MJ/kg \quad (10)$$

The heat content of pyrogenic water was included in the thermal effect, while the heat content of pyrolysis gas was determined, as with the energy yield coefficient, from the heat balance. To experimentally determine the pyrolysis gas composition and the yield of liquid products in time, the experimental devices shown in Figures 2 and 3 were used, respectively. For the experiments, the raw material was ground in a VLM-25 laboratory mill (Vilitek, Moscow, Russia) and screened through the Analysette 3 SPARTAN vibrating sieve (Fritsch, Idar-Oberstein, Germany) in order to separate the 0.2–1.0 mm fraction. The 20 g samples were loaded into the reactor and heated to 550 °C at a rate of 10 °C/min. Due to the small volume of the reactor working zone (653 cm^3), it was not purged with an inert gas before the experiment. The air contained in the reactor was displaced by water vapor released when heated to 120 °C. Within the temperature range of 200–550 °C, the volume of liquid products was measured for each 25 °C interval. The contents of the pyrolysis gas components, including CH_4, CO_2, CO, and H_2, were measured by means of the TEST-1 gas analyzer (BONER, Novosibirsk, Russia). The total volume of gas was calculated as a sum of the components by using TEST-1 for P20-004M (RS 232) gas analyzer software (Novosibirsk, Russia).

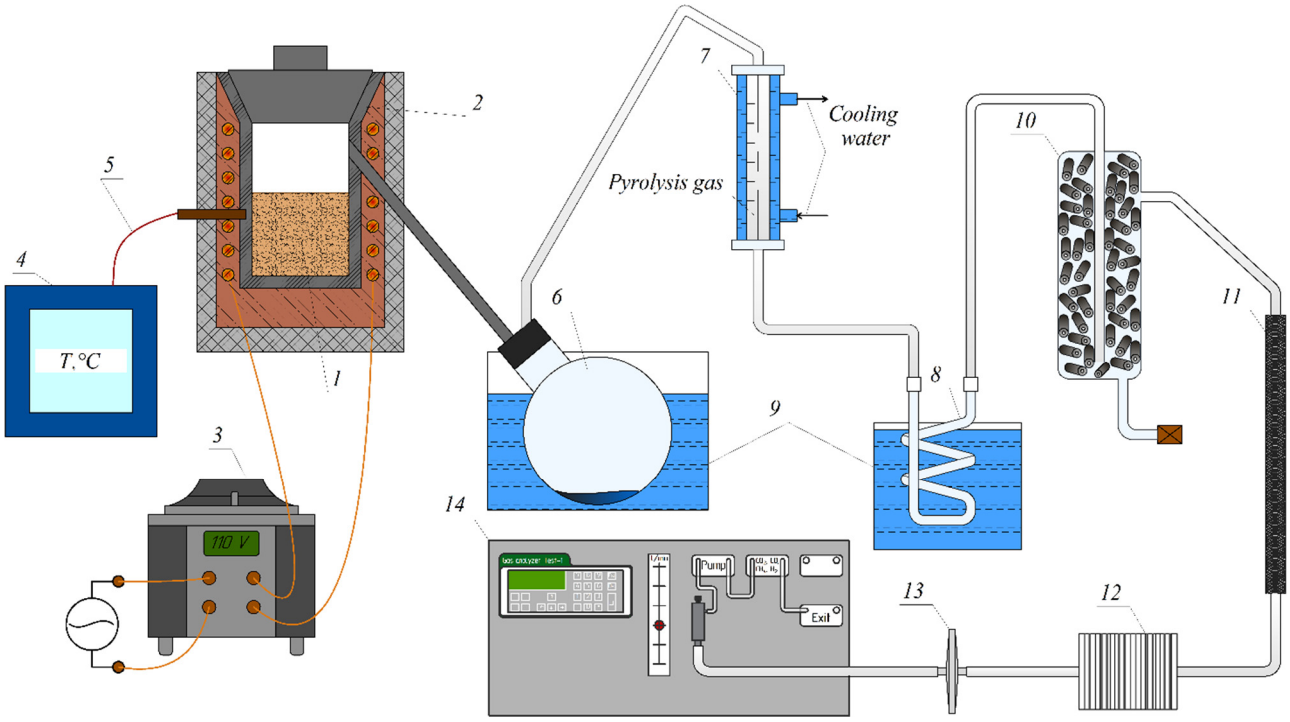


Figure 2. Laboratory device for the pyrolysis gas analysis: 1—Siberian pine nutshell, 2—reactor, 3—laboratory transformer, 4—high-precision multichannel temperature meter TM 5104 (Elemer, Moscow, Russia), 5—K-type thermocouple, 6—receiver flask, 7—down-flow condenser, 8—coiled condenser, 9—cooling water baths, 10—tubular filter, 11—activated-carbon filter, 12—cotton waste filter, 13—fluoroplastic filter, 14—gas analyzer TEST-1 (BONER, Novosibirsk, Russia).

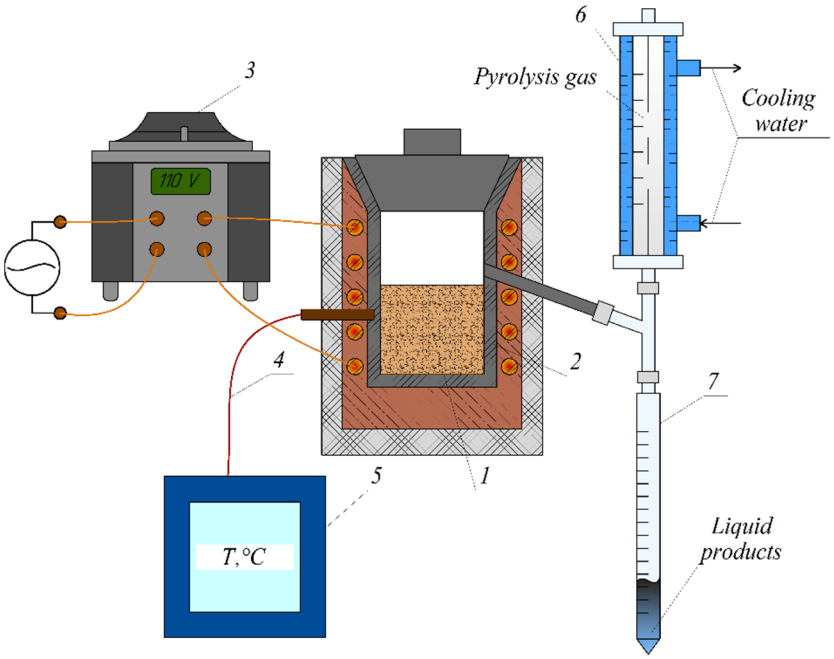


Figure 3. Laboratory device for measuring the yield of the liquid products in time: 1—Siberian pine nutshell, 2—reactor, 3—laboratory transformer, 4—high-precision multichannel temperature meter TM 5104 (Elemer, Moscow, Russia), 5—K-type thermocouple, 6—down-flow condenser, 7—gauged condensate collector.

3. Results and Discussion

The material balance is the primary and inalienable factor when studying the pyrolysis process. The balance, in the first approximation, provides the total heat of the process on the basis of component heat capacities. Hosokai et al. [50] studied the pyrolysis of cedar wood in a fluidized bed, determining the yield ratios between solid, liquid, and gaseous products, with the total heat generation of the process being positive.

Figure 4a shows the material balance of the Siberian pine nutshell pyrolysis. Based on the results, including those in Table 1, the energy shares among the pyrolysis products relative to the initial biomass are shown in Figure 4b.

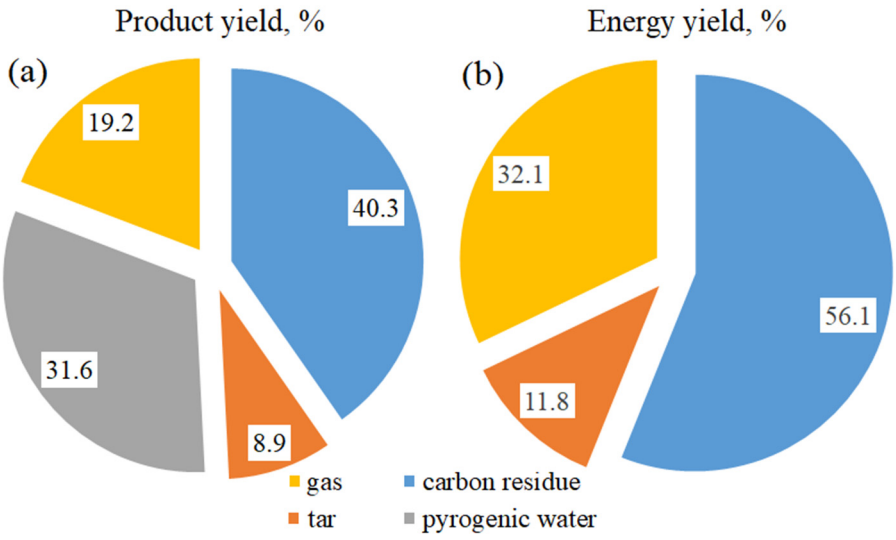


Figure 4. Material (**a**) and energy balance (**b**) of pyrolytic products.

The results confirm the promising properties of the biochar solid residue. It has the highest quantitative and energy yields relative to the initial biomass among the products. The pyrolysis gas also has a high share of energy yield.

The TG-DSC analysis of the pyrolytic processing of nutshell was carried out with the results given in Figure 5.

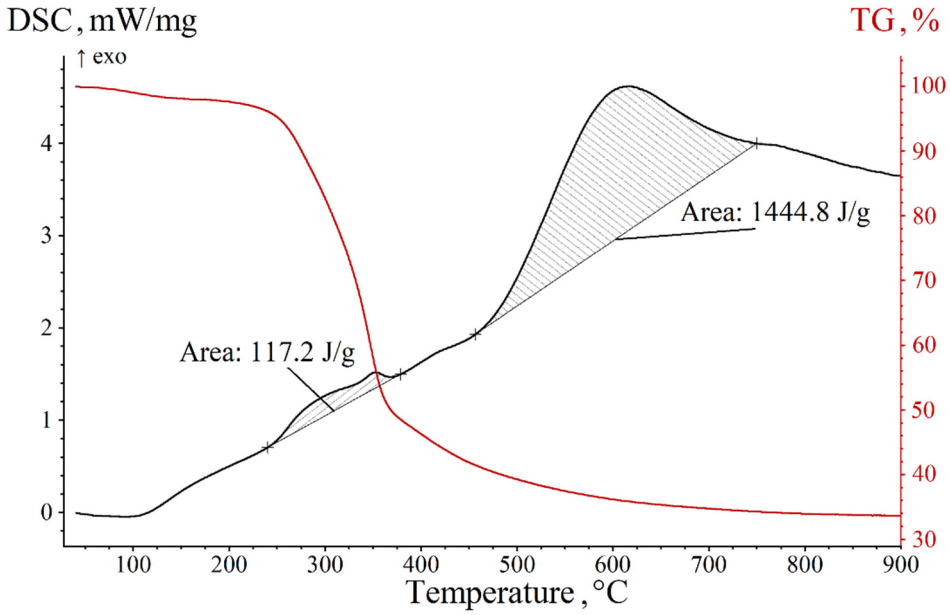


Figure 5. Results of the TG/DSC analysis of Siberian pine nutshell at a heating rate of 10 °C/min.

The heating of the raw material from ambient temperature to 120 °C resulted in the DSC showing an endothermic minimum associated with the evaporation of external moisture. Further heating brought an exothermic maximum within the temperature range of 250–370 °C, in which the organic part of the biomass decomposed, with the formation of volatile products comprising 45.8% of the initial mass of the raw material. In the temperature range of 470–750 °C, the second exothermic maximum appeared, with an insignificant mass loss of 6.6%.

The temperature range of the first exothermic maximum corresponded to the decomposition of cellulose and hemicellulose. A large share of the raw material decomposition was explained by the liquid and gaseous products formed in relative amounts of 85% and 90%, respectively [51]. The lignin decomposition proceeded evenly over the temperature range from 200 to 540 °C and, according to Yang et al. [19], could have proceeded even up to 900 °C under certain process conditions. With the lignin decomposition, exothermic reactions also took place due to the biochar structure rearrangement after releasing the major part of the volatile products, which can be seen in the slight decrease in the sample mass at the TG curve (Figure 5).

Analyzing the deviations from the DSC curve, one can see that the second exothermic maximum was significantly higher than the first maximum. This indicates a greater contribution of the thermal lignin transformation to the total thermal effect of pyrolysis. This assumption is substantiated by the fact that the area of the first exothermic maximum, at a lower temperature, was approximately thirteen times smaller than the second, i.e, the higher temperature one. At the same time, the cellulose and hemicellulose decomposition, according to the published data [19], almost completely ended before the temperature reached at the beginning of the second maximum (470 °C). Further heating and the resulting heat release were accompanied by the loss of mass during the lignin transformation. In addition, exothermic reactions were associated with changes in the structure of the carbonaceous residue, also mostly formed during lignin decomposition [52]. This fact is in good agreement with the observations of Chen et al. [31]; they reported the thermal effect

of secondary decomposition reactions of wood and straw as lignocellulosic biomass being almost an order of magnitude greater than that of cellulose, mainly decomposed below 400 °C.

The TG/DSC analysis (Figure 6) shows the total heat release of the exothermic reactions relative to 1 kg of dry raw material, together with the pyrolysis heat expenses at different process temperatures (Table 2).

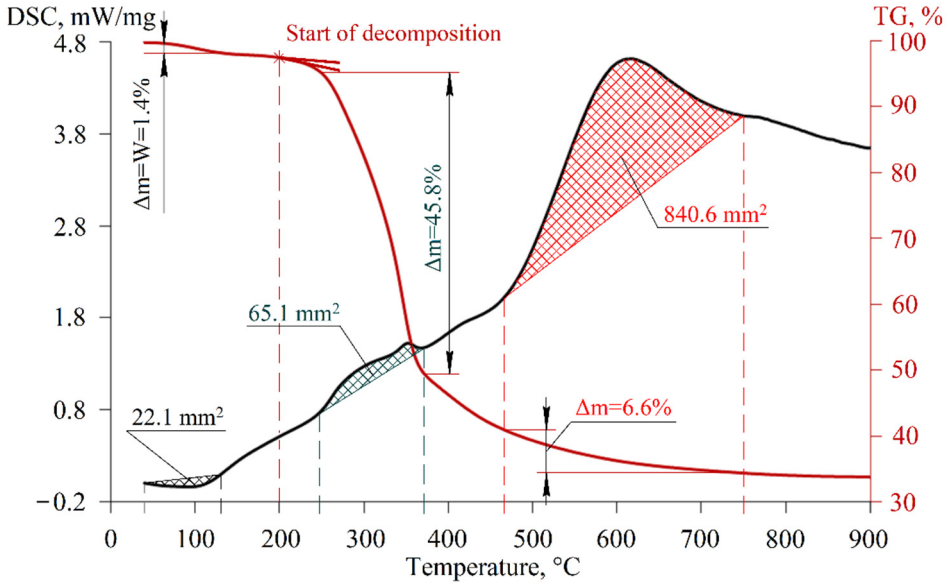


Figure 6. Numerical analysis of the TG/DSC results.

Table 2. Siberian pine nutshell pyrolysis: heat expenses and exothermic effects dependent on temperature.

Thermodynamic Characteristics of the Nutshell				Pyrolysis Temperature t_p, °C		
				550	650	750
t_1, °C	C_{p_b}, kJ/(kg·°C)	$C_{p_{cr}}$, kJ/(kg·°C)	' $C_{p_{vol}}$, kJ/(kg·°C)	Exothermic heat Q_{exo}, kJ/kg		
				345.4	1224.6	1557.8
200	2.1	1.7	1.96	Heat expense, kJ/kg		
				999.4	1179.5	1364.2

Endothermic and exothermic pyrolysis heat effects were assessed using Equations (11) and (12) (see also Equations (5) and (6)):

$$Q_{endo} = 4.187 \times \frac{1.4}{100} \times (120 - 20) + \frac{1.4}{100} \times 2258.2 = 37.5 \text{ kJ/kg} \quad (11)$$

$$Q_{exo} = 37.5 \times \frac{905.76}{22.10} \times \frac{100}{100 - 1.4} = 1557.8 \text{ kJ/kg} \quad (12)$$

The exothermic effect observed in the experiment is consistent with the one obtained by the NETZSCH Proteus instrument software (Figure 5), equal to 1562 kJ/kg. The heat released from exothermic reactions due to the decreased final pyrolysis temperature was calculated in a similar way: Table 2 presents the parameters and the results of the heat effect calculation for Siberian pine nutshell pyrolysis dependent on the final temperature. Comparing the pyrolysis heat expense with its exothermic release, one can conclude that the full coverage of heat expenses with an exothermic final process was achieved at 650 °C and above.

It should be noted that the Q_{exo} value also includes the heat of the reactions of pyrogenic water formation within the exothermic heat peak temperature ranges, together comprising a joint sector in the compiled heat balance (Figure 7).

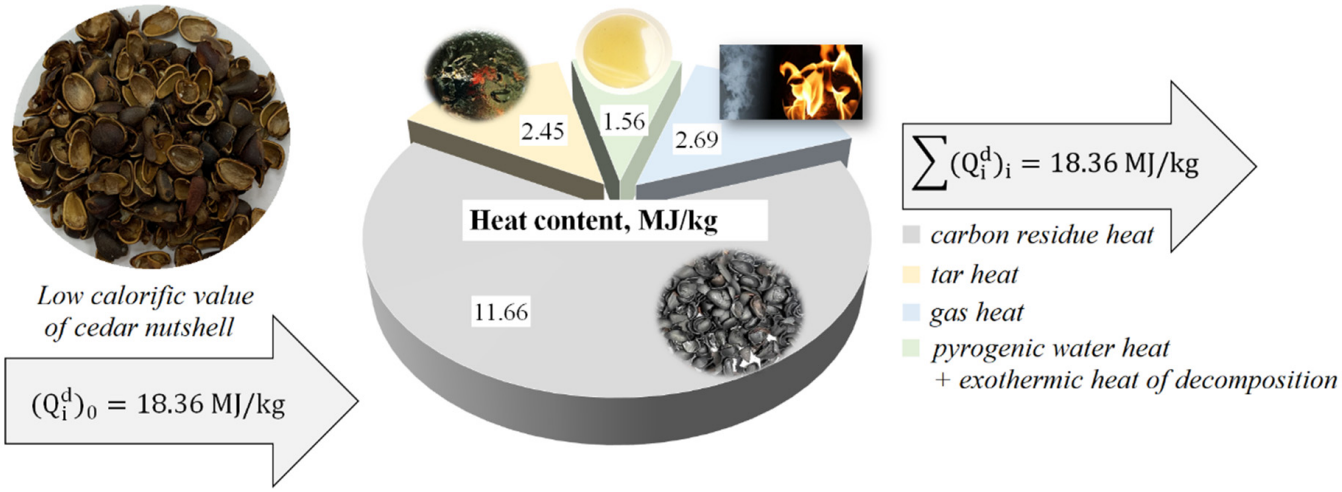


Figure 7. Thermal balance of Siberian pine nutshell pyrolysis.

At a process temperature of 550 °C, the pyrolysis gas combustion served as an additional energy source covering the heat expense. This made the gas composition a factor determining the balance of thermal effects in the applied temperature ranges. For example, a high methane content supports the process' exothermic character. The formation of methane may be described by the exothermic reactions between hydrogen and the raw material carbon (Equation (13)) or carbon monoxide (Equation (14)) [50]. In addition, during the heat release, the following reactions of interaction between carbon monoxide with water (Equation (15)) can occur:

$$C(s) + 2H_2(g) = CH_4(g) + 74.90\ kJ/mol \quad (13)$$

$$CO(g) + 3H_2(g) = CH_4(g) + H_2O(g) + 206.17\ kJ/mol \quad (14)$$

$$CO(g) + H_2O(g) = H_2(g) + CO_2(g) + 41.15\ kJ/mol \quad (15)$$

The pyrolysis gas composition was determined using quadrupole mass spectrometry, with the results given in Figure 8.

High yields were observed for carbon-containing gases (CO, CO_2, and CH_4) at 250–400 °C, as well as for hydrogen above 600 °C. The peak and practically the only release of carbon oxides occurred in the temperature range typical for the first exothermic maximum; above 400 °C, no carbon oxides were observed. Methane generation was observed in a wider temperature range, with three maxima from 250 to 550 °C (Figure 8b). Combustible CH_4, H_2, and CO made the pyrolysis gas a source of energy with the amount of combustion heat assessed. For this, the contents of the combustible components were experimentally determined within the temperature range up to 550 °C.

Figure 9 shows the Siberian pine nutshell pyrolysis gas composition, as well as the yields of liquid products at each temperature range, given relative to their total amount. The results are consistent with the analytical studies (Figure 8) in terms of temperature ranges for maximum liquid product release, as well as the concentrations of the considered gas components.

One can see the maximum CO and CO_2 concentrations in the pyrolysis gas, 29.0 and 46.6 vol.%, respectively, occurring between 325 and 375 °C, which coincides with the highest yield of liquid products within the first exothermic maximum temperature interval (Figure 5): at these temperatures, cellulose and hemicellulose decompose to produce pyrogenic water and levoglucosan formed from the pyrolysis of carbohydrates, with a

large share in the pyrolysis tar [53]. A large amount of CO and CO_2 in the pyrolysis gas was formed during the cracking and reforming of the C=O, COOH, and C-O-C groups in the biomass molecules [51]. With the temperature increased above 375 °C, the CO and CO_2 concentrations decreased, as well as the yield of liquid products. The rather high CO_2 concentration of 15 vol.% until the end of pyrolysis is explained by the carbon dioxide released from the char formation reactions [33]. The growth in methane concentration up to 43.2 vol.% at 480 °C corresponds to the initial stage of the second exothermic maximum, typically attributable to lignin decomposition with small amounts of water formed together with tar at 375–400 °C; this was also observed in this study [51].

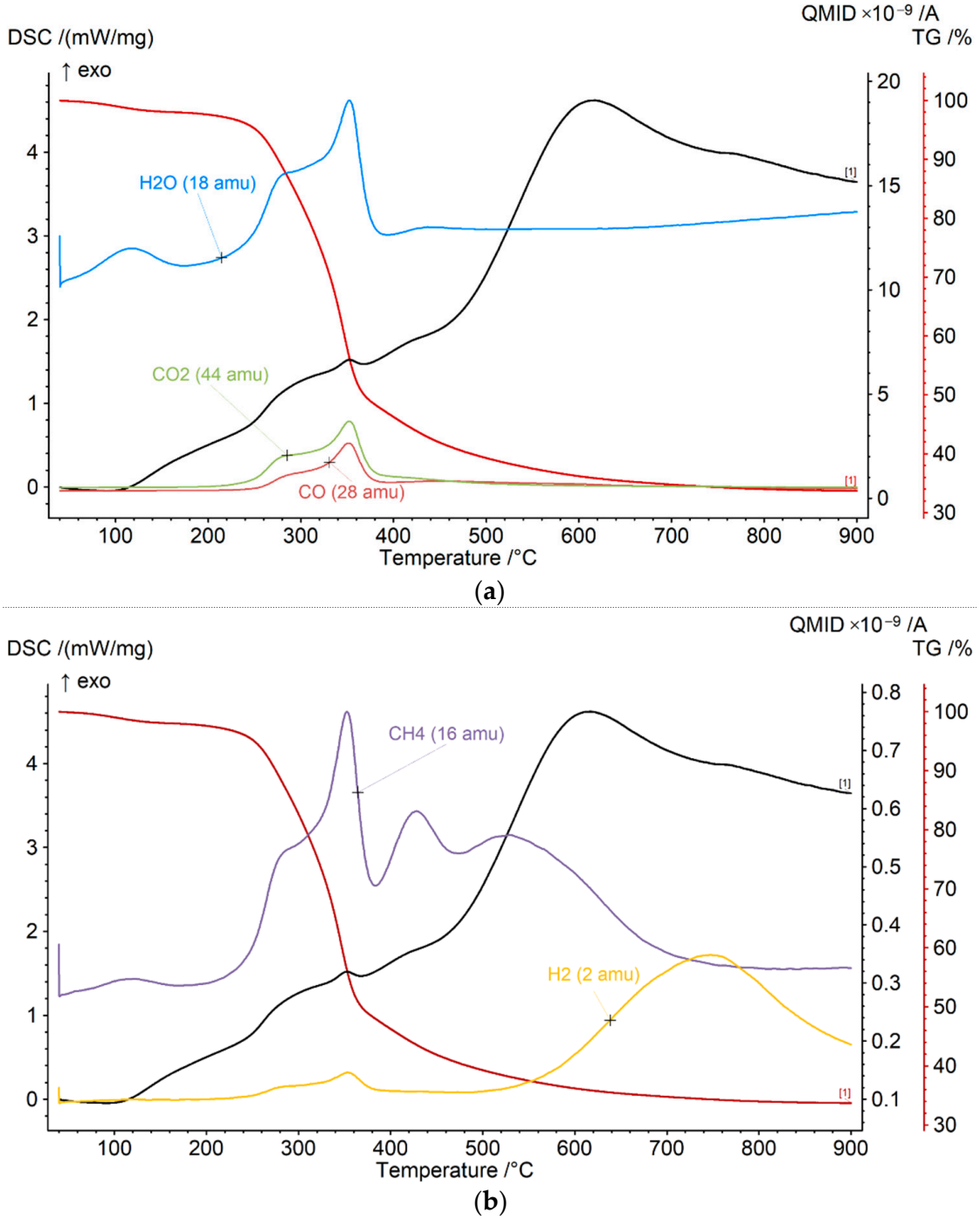


Figure 8. The pyrolysis gas composition in respect of water vapor, carbon monoxide, and carbon dioxide (**a**), and methane and hydrogen (**b**).

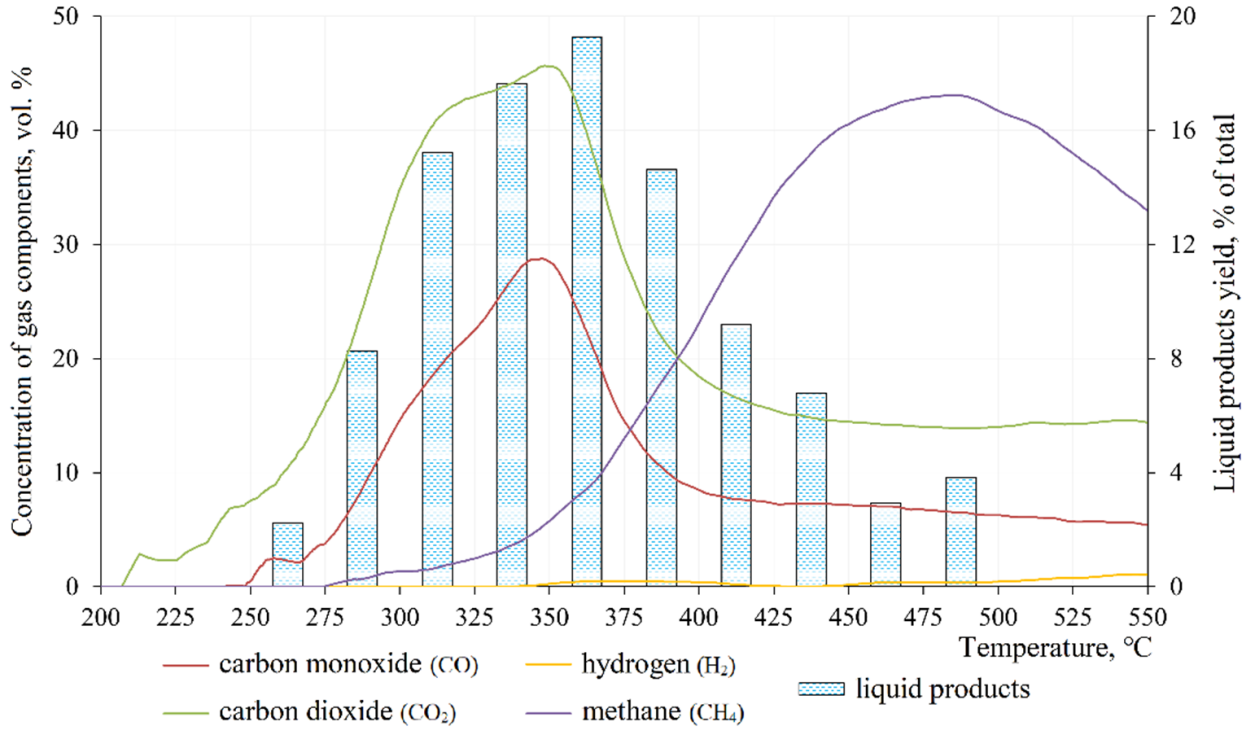


Figure 9. Pyrolysis gas composition and yields of liquid products in processing the Siberian pine nutshell.

Table 3 summarizes the average combustion heat values for the pyrolysis gas and the total volumes of combustible components (CO, H_2, and CH_4) relative to 1 kg of the raw material within the indicated temperature ranges. The multiplication of these data gives the total amount of heat obtained by the combustion of the gas, equal to $847.7 \cdot 10^{-3}$ MJ/kg (847.7 kJ/kg), which, together with exothermic reactions, covered the pyrolysis heat expense, thus setting up the prospects for pyrolysis gas utilization.

Table 3. The volumes and combustion heat of the pyrolysis gas combustible components relative to the Siberian pine nutshell mass.

Temperature Range ΔT, °C	Calorific Value Q_{mean}, MJ/m^3	Gas Yield V, m^3/kg	Gas Combustion Heat Q, MJ/kg
250–300	0.97	0.74×10^{-3}	0.7×10^{-3}
300–350	4.11	6.08×10^{-3}	25.0×10^{-3}
350–400	7.40	8.49×10^{-3}	62.8×10^{-3}
400–450	13.57	13.20×10^{-3}	179.1×10^{-3}
450–500	16.10	19.68×10^{-3}	316.9×10^{-3}
500–550	14.12	18.64×10^{-3}	263.2×10^{-3}
Total value	N.a.	66.83×10^{-3}	847.7×10^{-3}

N.a.—not applicable.

4. Conclusions

The pyrolysis heat expense may be covered by the inherent heat released in the thermal transformations of cellulose, hemicellulose, and lignin, which is characteristic of all plant biomass. The example of Siberian pine nutshell confirms the possibility of such heat coverage, with exothermic reactions at 650 °C in which the heat of 1224.6 kJ/kg exceeded the heat expense of 1179.5 kJ/kg. Exothermic reactions at a temperature range of 250–370 °C provided liquid products with CO_2 prevalence in the pyrolysis gas. At higher temperatures,

a positive thermal effect was associated with minimal weight loss. The large content of lignin in Siberian pine nutshell resulted in a high yield of methane in the pyrolysis gas, making its heat of combustion as high as 16.1 MJ/m^3 if formed within the temperature range of 450–500 °C. The combustion of gas formed from 1 kg of Siberian pine nutshell up to a temperature of 550 °C provided heat in the amount of 847.7 kJ, covering, together with the exothermic reactions, the pyrolysis heat expense. The method of assessing the coverage of heat expense developed in this research for the pyrolysis process may also be applied to the analysis of other types of biomass.

Author Contributions: Conceptualization, A.A., R.T. and I.S.; methodology, A.A. and R.T.; investigation, A.A. and K.I.; writing—original draft preparation, A.A. and I.S.; visualization, A.A. and K.I.; writing—review and editing, S.P.; project administration, R.T. All authors have read and agreed to the published version of the manuscript.

Funding: This work was supported by the Russian Foundation for Basic Research (grant number 20-38-90180). The pyrolytic processing of Siberian pine nutshell was experimentally implemented within the framework of the Russian Science Foundation project (22-19-00410 "Development of scientific and technical fundamentals of technology for obtaining microwave pyrolysis products from bio-coal compositions").

Institutional Review Board Statement: Not applicable.

Informed Consent Statement: Not applicable.

Data Availability Statement: Not applicable.

Conflicts of Interest: The authors declare no conflict of interest.

References

1. Chen, L.; Msigwa, G.; Yang, M.; Osman, A.I.; Fawzy, S.; Rooney, D.W.; Yap, P.S. Strategies to Achieve a Carbon Neutral Society: A Review. *Environ. Chem. Lett.* **2022**, *20*, 2277–2310. [CrossRef] [PubMed]
2. Huang, M.T.; Zhai, P.M. Achieving Paris Agreement Temperature Goals Requires Carbon Neutrality by Middle Century with Far-Reaching Transitions in the Whole Society. *Adv. Clim. Chang. Res.* **2021**, *12*, 281–286. [CrossRef]
3. Cheng, Y.; Sinha, A.; Ghosh, V.; Sengupta, T.; Luo, H. Carbon Tax and Energy Innovation at Crossroads of Carbon Neutrality: Designing a Sustainable Decarbonization Policy. *J. Environ. Manag.* **2021**, *294*, 112957. [CrossRef]
4. Paris Agreement, Paris. 2015. Available online: https://unfccc.int/process-and-meetings/the-paris-agreement/the-paris-agreement (accessed on 10 June 2022).
5. Framework for Attaining Carbon Neutrality in the United Nations Economic Commission for Europe (ECE) Region by 2050 Note by the Task Force on Carbon Neutrality. 2020. Available online: http://www.unece.org/energy/pathwaystose.html (accessed on 10 June 2022).
6. Shahbaz, M.; AlNouss, A.; Ghiat, I.; Mckay, G.; Mackey, H.; Elkhalifa, S.; Al-Ansari, T. A Comprehensive Review of Biomass Based Thermochemical Conversion Technologies Integrated with CO_2 Capture and Utilisation within BECCS Networks. *Resour. Conserv. Recycl.* **2021**, *173*, 105734. [CrossRef]
7. Krylova, A.Y.; Gorlov, E.G.; Shumovskii, A.V. Production of Biocoal by the Pyrolysis of Biomass. *Solid Fuel Chem.* **2019**, *53*, 369–376. [CrossRef]
8. Szufa, S.; Wielgosiński, G.; Piersa, P.; Czerwińska, J.; Dzikuć, M.; Adrian, Ł.; Lewandowska, W.; Marczak, M. Torrefaction of Straw from Oats and Maize for Use as a Fuel and Additive to Organic Fertilizers—TGA Analysis, Kinetics as Products for Agricultural Purposes. *Energies* **2020**, *13*, 2064. [CrossRef]
9. Malico, I.; Nepomuceno Pereira, R.; Gonçalves, A.C.; Sousa, A.M.O. Current Status and Future Perspectives for Energy Production from Solid Biomass in the European Industry. *Renew. Sustain. Energy Rev.* **2019**, *112*, 960–977. [CrossRef]
10. Ipiales, R.P.; de La Rubia, M.A.; Diaz, E.; Mohedano, A.F.; Rodriguez, J.J. Integration of Hydrothermal Carbonization and Anaerobic Digestion for Energy Recovery of Biomass Waste: An Overview. *Energy Fuels* **2021**, *35*, 17032–17050. [CrossRef]
11. Ruis, S.J.; Blanco-Canqui, H.; Creech, C.F.; Koehler-Cole, K.; Elmore, R.W.; Francis, C.A. Cover Crop Biomass Production in Temperate Agroecozones. *Agron. J.* **2019**, *111*, 1535–1551. [CrossRef]
12. Amenaghawon, A.N.; Anyalewechi, C.L.; Okieimen, C.O.; Kusuma, H.S. Biomass Pyrolysis Technologies for Value-Added Products: A State-of-the-Art Review. *Environ. Dev. Sustain.* **2021**, *23*, 14324–14378. [CrossRef]
13. González, R.; González, J.; Rosas, J.G.; Smith, R.; Gómez, X. Biochar and Energy Production: Valorizing Swine Manure through Coupling Co-Digestion and Pyrolysis. *C-J. Carbon Res.* **2020**, *6*, 43. [CrossRef]
14. Hoang, A.T.; Ong, H.C.; Fattah, I.M.R.; Chong, C.T.; Cheng, C.K.; Sakthivel, R.; Ok, Y.S. Progress on the Lignocellulosic Biomass Pyrolysis for Biofuel Production toward Environmental Sustainability. *Fuel Process. Technol.* **2021**, *223*, 106997. [CrossRef]

15. Wu, K.; Wu, H.; Zhang, H.; Zhang, B.; Wen, C.; Hu, C.; Liu, C.; Liu, Q. Enhancing Levoglucosan Production from Waste Biomass Pyrolysis by Fenton Pretreatment. *Waste Manag.* **2020**, *108*, 70–77. [CrossRef] [PubMed]
16. Roberts, A.F. The Heat of Reaction during the Pyrolysis of Wood. *Combust. Flame* **1971**, *17*, 79–86. [CrossRef]
17. Van de Velden, M.; Baeyens, J.; Brems, A.; Janssens, B.; Dewil, R. Fundamentals, Kinetics and Endothermicity of the Biomass Pyrolysis Reaction. *Renew. Energy* **2010**, *35*, 232–242. [CrossRef]
18. Kung, H.C.; Kalelkar, A.S. On the Heat of Reaction in Wood Pyrolysis. *Combust. Flame* **1973**, *20*, 91–103. [CrossRef]
19. Yang, H.; Yan, R.; Chen, H.; Lee, D.H.; Zheng, C. Characteristics of Hemicellulose, Cellulose and Lignin Pyrolysis. *Fuel* **2007**, *86*, 1781–1788. [CrossRef]
20. Fagbemi, L.; Khezami, L.; Capart, R. Pyrolysis Products from Different Biomasses: Application to the Thermal Cracking of Tar. *Appl. Energy* **2001**, *69*, 293–306. [CrossRef]
21. Lishtvan, I.; Dudarchik, U.; Kraiko, V. Energy and Technology Use of Biomass. *Proc. Natl. Acad. Sci. Belarus Chem. Ser.* **2016**, *4*, 91–101.
22. Mohan, D.; Pittman, C.U.; Steele, P.H. Pyrolysis of Wood/Biomass for Bio-Oil: A Critical Review. *Energy Fuels* **2006**, *20*, 848–889. [CrossRef]
23. He, F.; Yi, W.; Bai, X. Investigation on Caloric Requirement of Biomass Pyrolysis Using TG–DSC Analyzer. *Energy Convers. Manag.* **2006**, *47*, 2461–2469. [CrossRef]
24. Müsellim, E.; Tahir, M.H.; Ahmad, M.S.; Ceylan, S. Thermokinetic and TG/DSC-FTIR Study of Pea Waste Biomass Pyrolysis. *Appl. Eng.* **2018**, *137*, 54–61. [CrossRef]
25. Anca-Couce, A.; Scharler, R. Modelling Heat of Reaction in Biomass Pyrolysis with Detailed Reaction Schemes. *Fuel* **2017**, *206*, 572–579. [CrossRef]
26. Haseli, Y.; van Oijen, J.A.; de Goey, L.P.H. Modeling Biomass Particle Pyrolysis with Temperature-Dependent Heat of Reactions. *J. Anal. Appl. Pyrolysis* **2011**, *90*, 140–154. [CrossRef]
27. Vyrodov, V.A.; Kislicyn, A.N.; Gluhareva, M.I. *Tekhnologiya Lesohimicheskih Proizvodstv [Technology of Forest Chemical Production]*; Forestry Industry: Moscow, Russia, 1987; 352p.
28. Aronov, S.G.; Nesterenko, L.L. *Himiya Tverdyh Goryuchih Iskopaemyh [Chemistry of Solid Combustible Minerals]*; Kharkiv University: Kharkiv, Ukraine, 1960; 371p.
29. Di Blasi, C.; Galgano, A.; Branca, C. Exothermic Events of Nut Shell and Fruit Stone Pyrolysis. *ACS Sustain. Chem. Eng.* **2019**, *7*, 9035–9049. [CrossRef]
30. Timerbaev, N.F.; Safin, R.G.; Husnullin, I.I. Sovremennoe Sostoyanie Processa Pirogeneticheskoj Pererabotki Organicheskih Veshchestv [The Current State of the Process of Pyrogenetic Processing of Organic Substances]. *Bull. Kazan Technol. Univ.* **2011**, *3*, 169–174.
31. Chen, Q.; Yang, R.; Zhao, B.; Li, Y.; Wang, S.; Wu, H.; Zhuo, Y.; Chen, C. Investigation of Heat of Biomass Pyrolysis and Secondary Reactions by Simultaneous Thermogravimetry and Differential Scanning Calorimetry. *Fuel* **2014**, *134*, 467–476. [CrossRef]
32. Di Blasi, C.; Galgano, A.; Branca, C.; Clemente, M. Analysis of the Interactions between Moisture Evaporation and Exothermic Pyrolysis of Hazelnut Shells. *Energy Fuels* **2016**, *30*, 7878–7886. [CrossRef]
33. Gomez, C.; Velo, E.; Barontini, F.; Cozzani, V. Influence of Secondary Reactions on the Heat of Pyrolysis of Biomass. *Ind. Eng. Chem. Res.* **2009**, *48*, 10222–10233. [CrossRef]
34. Basile, L.; Tugnoli, A.; Stramigioli, C.; Cozzani, V. Influence of Pressure on the Heat of Biomass Pyrolysis. *Fuel* **2014**, *137*, 277–284. [CrossRef]
35. Mok, W.S.L.; Antal, M.J.; Szabo, P.; Varhegyi, G.; Zelei, B. Formation of Charcoal from Biomass in a Sealed Reactor. *Ind. Eng. Chem. Res.* **1992**, *31*, 1162–1166. [CrossRef]
36. Stahlfeld, K.W.; Belmont, E.L. Carbon Foam Production from Lignocellulosic Biomass via High Pressure Pyrolysis. *J. Anal. Appl. Pyrolysis* **2021**, *156*, 105115. [CrossRef]
37. Kononov, G.N.; Zarubina, A.N.; Verevkin, A.N.; Zaytsev, V.D.; Chekunin, D.B. Wood as a Chemical Raw Material. History and Modernity. III. Wood Pyrolysis as Processing Method. *For. Bull.* **2021**, *25*, 126–141. [CrossRef]
38. Huang, Y.; Li, B.; Liu, D.; Xie, X.; Zhang, H.; Sun, H.; Hu, X.; Zhang, S. Fundamental Advances in Biomass Autothermal/Oxidative Pyrolysis: A Review. *ACS Sustain. Chem. Eng.* **2020**, *8*, 11888–11905. [CrossRef]
39. Polin, J.P.; Carr, H.D.; Whitmer, L.E.; Smith, R.G.; Brown, R.C. Conventional and Autothermal Pyrolysis of Corn Stover: Overcoming the Processing Challenges of High-Ash Agricultural Residues. *J. Anal. Appl. Pyrolysis* **2019**, *143*, 104679. [CrossRef]
40. Li, D.; Berruti, F.; Briens, C. Autothermal Fast Pyrolysis of Birch Bark with Partial Oxidation in a Fluidized Bed Reactor. *Fuel* **2014**, *121*, 27–38. [CrossRef]
41. Zhang, H.; Xiao, R.; Wang, D.; Cho, J.; He, G.; Shao, S.; Zhang, J. Hydrodynamics of a Novel Biomass Autothermal Fast Pyrolysis Reactor: Solid Circulation Rate and Gas Bypassing. *Chem. Eng. J.* **2012**, *181–182*, 685–693. [CrossRef]
42. Chen, X.; Zhang, H.; Xiao, R. Mobile Autothermal Pyrolysis System for Local Biomass Conversion: Process Simulation and Techno-Economic Analysis. *Energy Fuels* **2018**, *32*, 4178–4188. [CrossRef]
43. Vamvuka, D. Bio-Oil, Solid and Gaseous Biofuels from Biomass Pyrolysis Processes—An Overview. *Int. J. Energy Res.* **2011**, *35*, 835–862. [CrossRef]
44. Jerzak, W. Experimental and Thermodynamic Analyses of Trace Element Speciation during the Combustion of Ground Cedar Nut Shells. *Energy Fuels* **2017**, *31*, 1969–1979. [CrossRef]

45. Jerzak, W. The Effect of Combustion Temperature on the Composition of the Ash and Gas From Cedar Nut Shell Combustion. *Energy Sources Part A Recovery Util. Environ. Eff.* **2017**, *39*, 9–16. [CrossRef]
46. Zhang, Z.; He, F.; Zhang, Y.; Yu, R.; Li, Y.; Zheng, Z.; Gao, Z. Experiments and Modelling of Potassium Release Behavior from Tablet Biomass Ash for Better Recycling of Ash as Eco-friendly Fertilizer. *J. Clean. Prod.* **2018**, *170*, 379–387. [CrossRef]
47. Tabakaev, R.; Ibraeva, K.; Astafev, A.; Dubinin, Y.; Yazykov, N.; Zavorin, A.; Yakovlev, V. Thermal Enrichment of Different Types of Biomass by Low-Temperature Pyrolysis. *Fuel* **2019**, *245*, 29–38. [CrossRef]
48. Kosowska-Golachowska, M.; Gajewski, W.; Musiał, T. Determination of the Effective Thermal Conductivity of Solid Fuels by the Laser Flash Method. *Arch. Thermodyn.* **2014**, *35*, 3–16. [CrossRef]
49. Park, W.C.; Atreya, A.; Baum, H.R. Experimental and Theoretical Investigation of Heat and Mass Transfer Processes during Wood Pyrolysis. *Combust. Flame* **2010**, *157*, 481–494. [CrossRef]
50. Hosokai, S.; Matsuoka, K.; Kuramoto, K.; Suzuki, Y. Practical Estimation of Reaction Heat during the Pyrolysis of Cedar Wood. *Fuel Process. Technol.* **2016**, *154*, 156–162. [CrossRef]
51. Quan, C.; Gao, N.; Song, Q. Pyrolysis of Biomass Components in a TGA and a Fixed-Bed Reactor: Thermochemical Behaviors, Kinetics, and Product Characterization. *J. Anal. Appl. Pyrolysis* **2016**, *121*, 84–92. [CrossRef]
52. Demirbaş, A. Mechanisms of Liquefaction and Pyrolysis Reactions of Biomass. *Energy Convers. Manag.* **2000**, *41*, 633–646. [CrossRef]
53. Yu, J.; Paterson, N.; Millan, M. The Primary Products of Cellulose Pyrolysis in the Absence of Extraparticle Reactions. *Fuel* **2019**, *237*, 911–915. [CrossRef]